Supporting Information for

REDOR NMR Reveals Multiple Conformers for Protein Kinase C Ligand in a Membrane Environment

Hao Yang,[1,‡] Daryl Staveness,[2,‡] Steven M. Ryckbosch,[2,‡] Alison D. Axtman,[2] Brian A. Loy,[2] Alexander B. Barnes,[1] Vijay S. Pande,[2] Jacob Schaefer,[1,*] Paul A. Wender,[2,3,*] Lynette Cegelski[2,*]

[1]Department of Chemistry, Washington University in St. Louis, St. Louis, MO 63130, United States

[2]Department of Chemistry, Stanford University, Stanford, CA 94305, United States

[3]Department of Chemical and Systems Biology, Stanford University, Stanford, CA 94305, United States

[‡]These authors contributed equally to this work.

*Correspondence: wenderp@stanford.edu; cegelski@stanford.edu; jschaefer@wustl.edu

This pdf file includes:

Materials and Methods
Table S1 and S2
Figs. S1 to S5
References (1-33)

Materials and Methods

General Preparation Methods

Unless otherwise noted, all reactions were run under a nitrogen atmosphere in flame or oven dried glassware. Reactions were stirred using Teflon-coated magnetic stirrer bars. Reactions were monitored using thin layer silica gel chromatography (TLC) using 0.25 mm silica gel 60F plates with fluorescent indicator from Merck. Plates were visualized by treatment with UV, acidic *p*-anisaldehyde stain, or $KMnO_4$ stain with gentle heating. Products were purified by column chromatography using the solvent systems indicated. Silica gel 60, 230-400 mesh, was purchased from Fisher Scientific. When necessary, solvents and reagents were purified before use. Tetrahydrofuran (THF) and dichloromethane (CH_2Cl_2) were passed through an alumina drying column (Solv-Tek Inc.) using nitrogen pressure. Ethyl acetate (EtOAc), dichloromethane, and methanol (MeOH) for purification purposes were obtained from Fisher Scientific. Amine bases (Et_3N, pyridine) were distilled from CaH_2 under nitrogen. [^{3}H]-PDBu was obtained from American Radiolabeled Chemicals. All other reagents were purchased from commercial suppliers (Sigma-Aldrich, Fisher Scientific) and were either used as received without additional purification or were purified using standard methods.

Preparative HPLC was carried out using an acetonitrile (MeCN)/H_2O gradient using a Shimadzu Prominence system equipped with a Restek 18 column (5 µm, 21 x 250 mm). NMR spectra were measured on a Varian INOVA 500 (^{1}H at 500 MHz, ^{13}C at 125 MHz) or a Varian INOVA 600 MHz (^{1}H at 600 MHz, ^{13}C at 150 MHz) magnetic resonance spectrometer, as noted. ^{1}H chemical shifts are reported relative to the residual solvent peak (chloroform = 7.26 ppm) as follows: chemical shift (δ), (multiplicity (s = singlet, d = doublet, t = triplet, q = quartet, p = pentet, b = broad, *app* = apparent), integration, coupling constant(s) in Hz, proton ID [when available, designated by carbon number]). Proton assignments were made via 2D spectroscopy (COSY, HSQC and/or HMBC) or analogy. ^{13}C chemical shifts are reported relative to the residual deuterated solvent ^{13}C signals ($CDCl_3$ = 77.16 ppm). Infrared spectra were recorded on a Perkin-Elmer 1600 Series Fourier transform spectrometer (FTIR) and are reported in wavenumbers (cm^{-1}). Optical rotation data were obtained using a JASCO P-2000 Polarimeter are reported as $[\alpha]_D^T$ (*c* = grams/100 mL), where D indicates the sodium D line (589 nm) and T indicates temperature (all optical rotation values were obtained at ambient temperature, ca. 22-25 °C). Unless otherwise indicated, optical rotations are the average (± standard deviation) of 10 individual measurements. Optical rotations were not recorded for isomeric mixtures. High-

resolution mass spectra were obtained at the Vincent Coates Mass Spectrometry Laboratory, Stanford, CA 94305.

Materials for biological evaluation (buffer reagents, solvents, disposable equipment, etc.) were obtained from Fisher Scientific. Phosphatidylserine was obtained from Avanti Polar Lipids (bovine brain PS in chloroform) or the NOF corporation (DOPS-Na, bovine, solid), and vesicles were created (as described further below) using a Branson Sonifier. Synthetic peptide was obtained from Anaspec and was initially compared to a sample provided by Prof. Kazuhiro Irie to verify its viability. Radiation counts were measured on a Beckman-Coulter LS 6500 Multi-Purpose Scintillation Counter with the samples being suspended in RPI Bio-Safe II Biodegradable Counting Cocktail.

Synthesis of [^{13}C,$^{2}H_3$]Phorbol 12,13-Diacetate

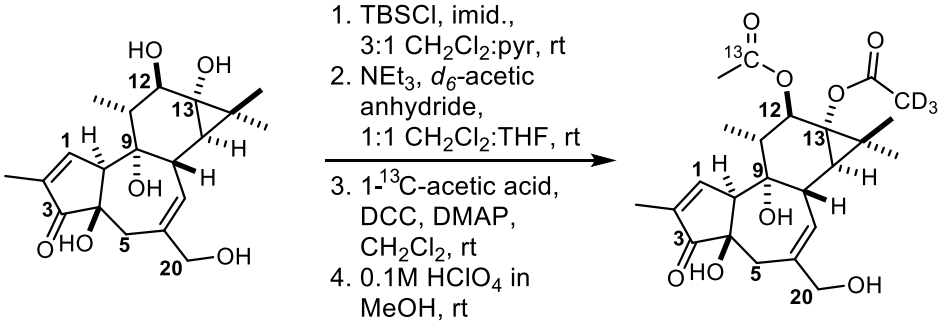

In a dry flask under an atmosphere of nitrogen, phorbol (**5**, 190 mg, 0.52 mmol) was dissolved in 2.6 mL dry CH_2Cl_2 and 1.3 mL pyridine (freshly distilled over CaH_2). Imidazole (160 mg, 2.3 mmol) was added in one portion. In a separate dry vial under N_2, TBSCl (120 mg, 0.78 mmol) was dissolved in 1.0 mL dry CH_2Cl_2. This solution was transferred into the phorbol/imidazole solution via syringe over the course of 1 minute. This transfer was quantified with 300 µL dry CH_2Cl_2. The reaction mixture became cloudy, and after 40 minutes stirring at room temp, the starting material was consumed as monitored by TLC. The reaction was concentrated under a stream of nitrogen; much of the pyridine remained after ~5 min. The resulting solution was transferred directly onto a silica column for purification by flash chromatography (1→8% MeOH:CH_2Cl_2, 1% increments, PhMe was used to load residual crude product). The product

was obtained as a slightly orange solid (184 mg) as a ~5:1 mix with what is believed to be the C4 α-epimer. This mixture was moved on without further purification.

A portion of the crude C20 TBS ether (31.2 mg) was dissolved in 650 µL dry THF and 650 µL dry CH_2Cl_2 in a dry vial under nitrogen. Triethylamine (91 µL, 0.65 mmol) and d_6-acetic anhydride (31 µL, 0.33 mmol) were added respectively in one portion each. The vial was flushed with Ar, capped, sealed, and stirred at room temp for 16 hrs before concentrating under a stream of nitrogen. The crude residue was purified via flash chromatography over silica (10→60% ethyl acetate:pentane, 10% increments, residue loaded with PhMe), providing 26.1 mg of a white solid that was moved on without further purification.

The C12-hydroxy, C13 d_3-acetate from above was dissolved in 750 µL dry CH_2Cl_2 in a dry vial under a nitrogenous atmosphere. DCC (36 mg, 0.18 mmol), 1-^{13}C-acetic acid (7.1 µL, 0.13 mmol), and DMAP (21 mg, 0.18 mmol) were added respectively, one portion each. After 4.5 hrs stirring in room temp, the cloudy reaction mixture was determined to be complete by TLC analysis. After concentration under a stream of nitrogen, the crude residue was purified with flash chromatography over silica (5→25% ethyl acetate:pentane, 5% increments, residue loaded with PhMe). The desired C12 ^{13}C-acetate was afforded as a white solid (24.1 mg).

The bis-acetylated C26 TBS ether was dissolved in 4.3 mL of a 0.1 M $HClO_4$ in dry MeOH in a dry vial, flushing with Ar after addition of acid. Full deprotection was achieved in 1.5 hrs at room temp as monitored by TLC. The reaction was quenched with 10 mL 1:1 sat. $NaHCO_3$ to H_2O and diluted with 10 mL ethyl acetate. The phases were separated, and the aqueous phase was extracted with four 10 mL portions of ethyl acetate. The combined organic phases were washed with 10 mL brine, dried over anhydrous sodium sulfate, filtered to remove solids, and concentrated under vacuum. The crude residue was purified by flash chromatography over silica (50 to 70 to 80 to 90% ethyl acetate:pentane, residue loaded with benzene). The white solid (22.1 mg) was further purified with reverse phase HPLC (50→100% MeCN:H_2O, 30 min, loaded product in 400 µL 3:1 MeOH:MeCN). The product was not highly soluble in the solvent mixture used to load, leaving 4.3 mg crude product in the original vial, and the gradient was too non-polar, eluting the product at ~3 min into the run. Despite these errors, this method provided 16.1 mg of pure [^{13}C,$^{2}H_3$]PDAc **4** as a white solid (40.3% over four steps).

Characterization data is provided below; ^{1}H and ^{13}C NMR spectra are provided as Figures S4 and S5. The K_i for full-length PKCδ (supplied by Life Technologies) was determined to be 11 nM (95% confidence interval = 7.0-17 nM; R^2 = 0.98) by a filtration-based heterogeneous competitive binding assay with [^{3}H]PDBu (see next section).

*Characterization Data for [^{13}C, $^{2}H_3$]PDAc **4**:*

^{1}H NMR ($CDCl_3$, 500 MHz): δ = 7.56 (s, 1H, C1), 5.67 (d, 1H, *J* = 5.4 Hz, C7), 5.58 (br s, 1H, C9-OH), 5.36 (dd, 1H, *J* = 10.5, 4.1 Hz, C12), 4.03 (d, 1H, *J* = 13.3 Hz, C20), 3.96 (d, 1H, *J* = 13.3 Hz, C20), 3.27-3.19 (m, 2H, C8, C10), 2.96 (br s, 1H, C4-OH), 2.58 (d, 1H, *J* = 19.1 Hz, C5), 2.47 (d, 1H, *J* = 19.1 Hz, C5), 2.18-2.11 (m, 1H, C11), 2.07 (d, 3H, *J* = 6.9 Hz, -$O_2{}^{13}CCH_3$), 1.75-1.73 (m, 3H, C19), 1.23 (s, 3H, C15-Me), 1.21 (s, 3H, C15-Me), 1.08 (d, 1H, *J* = 5.4 Hz, C14), 0.88 (d, 3H, *J* = 6.4 Hz, C18) ppm

^{13}C NMR ($CDCl_3$, 125 MHz): δ = 209.3, 174.0, 171.2 (^{13}C label), 160.9, 140.7, 133.0, 129.2, 78.4, 77.1, 73.8, 68.1, 65.7, 56.1, 43.0, 39.1, 38.6, 36.3, 25.9, 24.0, 21.2 (d, J_{13C-C} = 59.9 Hz), 16.8, 14.5, 10.2 ppm*.

IR (thin film): 3401, 2921, 1698, 1374, 1328, 1270, 1207, 1081, 1018, 909, 733 cm^{-1}

HRMS (ES+, *m/z)* calculated for $C_{23}\{^{13}C\}H_{29}D_3NaO_8^+$: 475.2211, Found: 475.2202

$[\alpha]_D^{22.9\,^{\circ}C}$ =96.0 ± 0.6° (*c* = 1.0, CH_2Cl_2)

R_f= 0.20 (70% EtOAc in pentane), one black spot, *p*-anisaldehyde + UV

* The CD_3 carbon signal could not be detected, likely due to the ^{2}H-based splitting and long relaxation time.

Ligand Binding Assay and Preparation of Materials

A radioligand binding assay using [^{3}H]PDBu (similar to that previously described[1,2]) was employed to assess the binding activity of the PKCδ-C1b peptide in various conditions in order to determine the best conditions for NMR sample preparations.

PKCδ-C1B peptide. Five mol. equivalents of 5 mM $ZnCl_2$ in ultrapure water were added to a 208 μM aqueous solution of the mouse PKCδ-C1b peptide (HRFKVYNYMSPTFCDHCGSLLWGLVKQGLKCEDCGMNVHHKCREKVANLCG), corresponding to residues 231-281 of full-length mouse PKCδ. The resultant 172 μM solution was allowed to stand on ice for 10 min. The PKCδ-C1b peptide solution was distributed to 1.5 mL-Eppendorf tubes [each with 10 μL (1.72 nmol) or 5 μL (0.86 nmol)] and stored at -80ºC until

use. Just before use, an individual aliquot was thawed on ice and diluted to 1.72 μM with chilled ultrapure water. This solution was used immediately and became non-functional within several hours of dilution regardless of storage temperature.

Phosphatidylserine (PS) multilamellar vesicles (MLVs). PS [L-α-phosphatidylserine sodium salt (Brain, Porcine) (Avanti Polar Lipids)] was obtained as a 10 mg/mL solution in chloroform. A 175 μL aliquot was transferred to a conical vial and concentrated under a stream of nitrogen. The PS was then stored under vacuum for at least 10 minutes before resuspending in 1.75 mL 50 mM Tris-maleate buffer pH 7.4 and placed on ice. Sonication was performed using a needle-nose sonicator (Branson Sonifier 250, power = 6, 40% duty cycle) in six cycles of 30 seconds sonication:30 seconds rest on ice. The cloudy mixture was stored on ice for single-day use and could be scaled as needed for additional assays.

[^{3}H]PDBu (American Radiolabeled Chemicals). One 50 μCi ampoule containing 20 Ci/mmol [^{3}H]PDBu in acetone was dried completely under a stream of nitrogen and then stored under vacuum. The residue was resuspended in DMSO to a concentration of 2.0 μM and stored at -20 ºC until use.

K_d Determinations

The following was added to a 1.5 mL polypropylene microcentrifuge tube stored on ice: 155.5 μL 50 mM Tris-maleate buffer pH 7.4 ("buffer"); 75 μL 10 mg/mL bovine γ-globulin in buffer; DMSO; 12.5 μL 1 mg/mL PS vesicles from above; [^{3}H]PDBu in DMSO; and 2.0 μL 1.72 μM PKCδ-C1b domain in water. Total DMSO volume was 5 μL. The ratio of DMSO to [^{3}H]PDBu solution was varied to generate the following concentrations (each done in triplicate): 0.1 nM, 0.2 nM, 0.4 nM, 0.8 nM, 1.6 nM, and 3.2 nM (concentration of [^{3}H]PDBu after addition of all components). The 2.0 μM stock of [^{3}H]PDBu was diluted to 0.2 μM for the 3 highest concentrations and 0.02 μM for the 3 lowest concentrations. Final solutions were incubated at room temperature for 10 min, and then on ice for 10 min. 187 μL of 0.54 g/mL PEG8000 in buffer was then added and the tube was vortexed vigorously. Solutions were then incubated on ice for 20 min and then centrifuged for 10 min at 12,000 rpm in an Eppendorf microcentrifuge at 4 ºC. A 50 μL aliquot of the supernatant of each sample was removed, and dissolved in 2 mL RPI Bio-Safe II Biodegradable Counting Cocktail. The radioactivity of these samples was defined as the free ligand (measured in cpm). The remainder of the supernatant of each tube

was removed by aspiration, and the tips of the tubes were cut off to access the pellets. Pellets were resuspended in 2 mL liquid scintillation cocktail via pipette. The radioactivity of the pellets was defined as the bound ligand (cpm). The K_d determination was then performed by Scatchard analysis in which the quotient of the bound ligand and free ligand were plotted as a function of the effective ligand concentration in nM. When run in triplicate, the bound values and free values were averaged independently and the averages were used to determine y-values. Following a linear fit of the data, the slope is equal to $-1/K_d$ and examining the R^2 value reveals the goodness of fit (Table S1).

Optimization of the Lipid:Peptide Ratio for NMR Sample Preparation

The influence of the lipid:peptide ratio was examined in order to select conditions for the NMR sample preparation that best recapitulate the behavior of ligand-bound peptide in the binding assay described above, and to maximize the NMR sensitivity of the experiment by employing the highest peptide content possible. Table S1 summarizes the results in varying lipid:peptide ratios. It appeared that a 50:1 ratio was the minimal amount of lipid that could be used while maintaining a high affinity for the ligand. It was also demonstrated that the cryoprotectant trehalose, necessary for vesicle integrity upon lyophilization, had no effect on binding.

NMR Sample Preparation

Large-scale lyophilized solid-state samples were prepared with the goal of obtaining 220 mg of final lyophilized sample to be loaded into a 5-mm thin-wall rotor. Components included in this sample were phosphatidylserine (PS, Avanti Polar Lipids), ligand ([^{13}C,^{2}H$_3$]PDAc, or [^{19}F,^{13}C,^{2}H$_3$]bryolog), peptide (Anaspec, PKCδ C1b domain), and trehalose (vesicle cryoprotectant). The sample was prepared using a molar ratio of 1:1:50:50 for ligand:peptide:PS:trehalose. Table S2 lists the components added in the order they were mixed. The order of addition corresponds exactly with that employed in the centrifugation assay.

A total volume of 55.8 mL was elected for sample preparation to maintain the peptide concentration normally employed (172 μM when folding the peptide for the centrifugation assay). Within this 55.8 mL, the volume was divided into its typical percentages of solvent, including 48% ultrapure water, 2% DMSO, and 50% 50 mM Tris-maleate buffer, according to the centrifugation assay protocol. Briefly, PS vesicles were prepared as described previously (needle-nose sonication) in a 50 mL falcon tube with the volume shown in Table S2. At the same time, a 4.12 mM stock solution of [^{13}C,^{2}H$_3$]PDAc **4** was prepared in DMSO (stored -20 ^{o}C

after use). Next, peptide was dissolved in 22.3 mL ultrapure water plus 4.6 mL 5.0 mM $ZnCl_2$ (23 μmol, 5 eq) and incubated on ice for 10 min. Ligand was added to the falcon tube containing PS vesicles, to which the folded peptide was then added. Following two 10-minute incubations, one at room temperature and the second on ice, the solution was divided and centrifuged at 50000g for 15 min. Resultant pellets were resuspended in 25 mM trehalose and combined in a single 15 mL falcon tube. After flash freezing using liquid N_2, the sample was lyophilized for more than 48 hours to ensure dryness. The lyophilized sample was packed into pellets and transferred to a thin-wall zirconia rotor fitted with Teflon spacers and a drive tip. The loaded rotor was stored at -20 ^oC until use. The preparation of the [^{19}F,^{13}C,$^{2}H_3$]bryolog sample for solid-state NMR followed the same protocol.

CPMAS and REDOR NMR Experiments

REDOR[3,4] was used to determine internuclear distances between ^{13}C and D_3 in PDAc and between ^{13}C, ^{19}F, and D_3 pairs in the bryolog. REDOR experiments are done in two parts, once with rotor-synchronized dephasing pulses (S) and once without (S_0). The dephasing pulses change the sign of the heteronuclear dipolar coupling, and this interferes with the spatial averaging from magic-angle spinning. The difference in signal intensity ($\Delta S = S_0 - S$) for the observed spin in the two parts of the REDOR experiment, scaled by S_0, is directly related to the corresponding distance to the dephasing spin.

The solid-state NMR spectrometer has an 89-mm bore, 12-T static field magnet (^1H at 500 MHz, Magnex, Agilent, Santa Clara, CA), a Tecmag (Houston, TX) Apollo console, and a homebuilt four-channel (^1H, ^{19}F, ^{13}C, ^{2}H) transmission-line probe equipped with a 5-mm Chemagetics/Varian stator and zirconia rotors. Radiofrequency pulses for ^1H and ^{19}F were amplified first by a 50-W American Microwave Technology (AMT, Anaheim, CA) power amplifier and then by a 2-kW Creative Electronics tube amplifier. AMT amplifiers (2 kW) were used for ^{13}C and ^{2}H pulses. In all the NMR experiments, 71 kHz pulses (7 μs for π pulses) were used for ^1H, ^{13}C and ^{2}H, and the proton decoupling strength was 80 kHz. 100 kHz pulses (5 μs for π pulses) were used for ^{19}F. Matched cross-polarization transfers were made at 71 kHz in 1.5 ms in the C{D}, C{F}, D{F} REDOR and ^{13}C CPMAS experiments. Adamantane was used as an external ^{13}C chemical shift reference.[5] Spinning rates were actively controlled to 7143±2 Hz. All RF pulse amplitudes were under active control (H_1 control) to eliminate long-term drifts due to component aging or changes in temperature.[6] Additionally, alternating scans of S_0 and S were

acquired to compensate for short-term drift. XY-8 phase cycling[7] was used for all refocusing and dephasing pulses.[8]

REDOR Calculations

REDOR dephasing for C-F and D_3-F systems was calculated using the analytical expression of Mueller et al. for spin-1/2 pairs.[9] REDOR dephasing for the C-D_3 system was calculated using modifications of the analytical expression for spin-1/2 pairs. A single C-D pair would exhibit maximum dephasing of 67%,[10] corresponding to two of the three eigen states (m=+1, 0, -1) for D that are spin-active (m=+/-1). There are 27 states for a D_3 group, where 7 states are not spin-active. Thus the maximum C-D_3 dephasing is 74% (20/27).[11] The dephaser in the phorbol diacetate is usually present as a CD_3 group, but some was present as CD_2 and CDH_2. Mass spectrometry determined the enrichment as 90.1% CD_3, 8.5% CD_2H, 0.6% CDH_2 and 0.8% CH_3. These values were included in the calculation and the corresponding maximum dephasing is 73% here. The rapidly rotating CD_3 dephaser was approximated as a single super spin centered in the triangle defined by the three ^2H nuclei.[11] Similarly, the CD_2H was treated as a super spin centered in the D_2H triangle, and the CDH_2 was treated as a single spin centered in the DH_2 triangle. For the calculation, a fit of $\Delta S/S_0$ as a function of dephasing time yielded the dipolar coupling constant and hence the internuclear distance.

Molecular Dynamics Simulations

Structure Preparation. The starting structures for molecular dynamics simulations of the PKCδ C1b-bryolog 1 complex and embedded in the membrane were taken from a recent study of ours examining the role of different ligands in the interactions of the PKCδ C1b-ligand complex with the membrane.[12] In this way, the starting structures of the bryostatin simulations were directly modified to convert into bryolog 1, replacing the C13 ester with a fluorine and the hydrogen germinal to the ester with an ester itself, and changing the C20 octadienoate into a saturated octanoate. Thus, the starting configuration was of the labelog bound to the PKCδ C1b domain and at various levels of penetration into a phospholipid membrane. Ligand parameters for all simulations were found using Antechamber and the general amber force field (GAFF),[13,14] and converted to gromacs format using acpype.[15] Lipid parameters were derived from the Stockholm lipid (Slipid) parameters.[16] The headgroup parameters of dioleoyl phosphatidylserine (DOPS) and the fatty acid parameters of palmitoyloleoylphosphatidylglycerol (POPG) were combined to

yield the palmitoyloleoyl phosphatidylserine (POPS) parameters which were used. A membrane of 128 POPS monomers was assembled using PACKMOL.[17]

Simulation details. All simulations were performed using GROMACS 4.5.3[18] on the distributed computing platform Folding@home.[19] The AMBER99SB-ILDN[20] force field was used for proteins, GAFF[13] for ligands, Slipids parameters for lipids, and TIP3P[21] for water. This system was then solvated in an orthorhombic box where the dimensions were set by the x and y lengths of the bilayer, and such that water extended at least 1 nm from any heavy atoms in the z direction; 127 waters were replaced with Na^+ ions to neutralize the charges on both the protein and the phospholipids for a total of ~35000 atoms for each of the systems. All simulations were run with a 2 fs timestep. Structures were minimized using steepest descent with a cutoff of 1000 kJ/(mol x nm). Pressure was controlled semi-isotropically using the Parrinello-Rahman barostat,[22] with a time constant of 10 ps, a reference pressure of 1 bar in both the x-y and z dimensions, and an isothermal compressibility of 4.5×10^{-5}/bar. All bonds were constrained using LINCS,[23] and long-range electrostatic interactions were treated using Particle-Mesh Ewald (PME),[24] with cubic interpolation and 0.12 nm grid spacing. Dispersion correction was turned off, as it was found to result in membranes with an unnaturally low area per lipid. Dispersion correction is best used in homogenous aqueous systems, not heterogeneous systems such as those including aqueous solvents and phospholipid membranes. The neighbor list was updated with a grid searching every 10 fs in all simulations. Short-range neighbor list, van der Waals, and electrostatic cutoffs were all set to 1.0 nm. Center-of-mass motions were removed independently for two groups (1: protein, zinc, lipids, and ligand, 2: waters and sodium). Periodic boundary conditions were used for all simulations and randomized starting velocities were assigned from a Maxwell-Boltzmann distribution. Each of the 930 starting configurations (each featuring a different depth and orientation of the peptide-ligand complex in the membrane) possessed 15 clones, and they were simulated in the NPT ensemble according to the parameters described above for a total of about 14000 trajectories per system and 40 ns per trajectory, adding up to ~560 μs of aggregate simulation time.

Data Analysis: Markov State Models*.* This dataset was then featurized using MSMBuilder 3.[25] Featurization is the process by which certain quantities particular to a system (such as the dihedral angles of the protein backbone) are aggregated from every relevant atom and every frame. This data (the system's "features") act as a way to describe the structure and dynamics of the system as a whole. Seven different featurizations were used to describe the system in

this study. Three featurizations were used to measure protein conformation through: (i) backbone dihedral angles, (ii) rmsd of the protein when superposed with a reference structure, and (iii) a distribution of reciprocal interatomic distances (DRID)[26] of all heavy atoms. Two featurizations measured the localization of water around the protein (the solvent shell featurizer[27] measures the local, instantaneous water density around all protein and ligand heavy atoms within a certain radius; in this case radii of 0.3 nm and 1.0 nm were used). The remaining two featurizations measured the localization of lipid molecules around the protein and ligand (one used the same solvent shell featurizer except using lipids instead of waters, and the other used a weighted metric measuring the distance of every protein heavy atom to every lipid phosphorus atom[28]). These seven featurizations were combined such that each new one consisted of 0 or 1 characterization of the protein, water, and lipid systems. This yielded a total of 35 different featurizations for future analysis.

On each of these featurizations, we performed a tICA analysis.[29] We measured the four most slowly decorrelating linear combinations of these features, using a tICA lag time, *t*, between 0.5 ns and 5 ns and an L2 regularization strength gamma, *g*, between 10^{-1} and 10^{-10}. These tICs were then clustered into *k* states using the mini-batch k-means clustering method.[30] Using this clustering, Markov state models (MSMs) were built using lagtime of 4.5 ns. In order to determine optimal values for *t*, *g*, and *k* of the model, we sought to maximize the eigenvalues of our MSM, in accordance with the variational formulation of kinetics introduced by Nüske and Noé.[31] However, we were also cognizant that overfitting, arising for example due to an overly large value for *k* or overly small of a value for *g*, could pose a risk. For this reason, we selected these values by cross-validation using the variational GMRQ objective function described by McGibbon and Pande,[32] which assesses how well the MSMs maximize a variational criterion evaluated on data that was held out during the fitting of the model. This optimization was managed by osprey (available at https://github.com/pandegroup/osprey), a tool for hyperparameter optimization of algorithms in machine learning.

Each iteration of the optimization involved building an MSM using a random subset of the data (the training set) and evaluating how slowly the first six eigenvectors of the MSM decorrelate when measured against the remaining subset of the data (the training set). Those that decorrelate the most slowly have the highest GMRQ scores and can be considered the “best” MSMs.

Data analysis: Free energy histograms. Histograms relating the free energy of the system were made by calculating the C-D, C-F, and D-F intramolecular distances. The free energy histograms themselves were made by summing over all states of the MSM using the following equation: $W(x) = k_B T \ln\left[\sum_i^N \pi_i h_i(x)\right]$, *W(x)* is the function describing this free energy histogram, *N* is the number of states in the given MSM, *x* is the intramolecular distance in question, π_i is the probability of state *i*, and $h_i(x)$ is the normalized histogram of *x* from within state *i* specifically.

Supplementary Tables

	1[a]	2	3	4	5	6	7[e]	8	10
Lipid:Peptide Ratio[b]	~4300:1	~4300:1	~4300:1	1000:1	250:1	125:1	**50:1**	40:1	20:1
Trehalose[c]	-	-	Y	Y	Y	Y	Y	Y	Y
K_d (nM)	**0.36**	**0.52**	**0.50**	**1.2**	**1.7**	**1.1**	**1.5**	**4.9**	**26**
R^2	0.94	0.99	0.98	0.92	0.93	0.97	0.99	0.89	0.87
95% CI (nM)[d]	0.20-1.4	0.38-0.81	0.39-0.71	0.64-15	0.93-11	0.73-2.6	1.2-2.1	n/a	n/a

Table S1: K_d values for screening NMR sample preparation conditions.

[a]Each column represents an individual experiment using the 0.1-3.2 nM concentration range described in the text in triplicate; [b]Lipid ratios varied by adding the appropriate amount of buffer to compensate for the amount of PS vesicle solution not added; [c]Trehalose was added directly to the 10 mg/mL γ-globulin solution in buffer to achieve an 83 mM solution (with respect to trehalose; which is 25 mM when all components are mixed); [d]95% confidence interval; [e]This ratio was chosen as the lowest tolerated lipid:peptide ratio and was used in all subsequent studies.

Component	**MW (g)**	**Amount (mg)**	**Moles (μmol)**	**Volume added**
PS	825.0	190.9	231	27.8 mL of 8.3 mM stock in 50 mM Tris-maleate buffer
[^{13}C,$^{2}H_3$]PDAc	452.5	2.1	4.6	1.13 mL of 4.12 mM stock in DMSO
Peptide (plus $ZnCl_2$)	5854.6	27.1	4.6	26.9 mL of 172 μM stock in ultrapure water
Trehalose	342.3	79.1	231	9.2 mL of 25 mM stock in ultrapure water

Table S2: Large-scale sample preparation.

Supplementary Figures

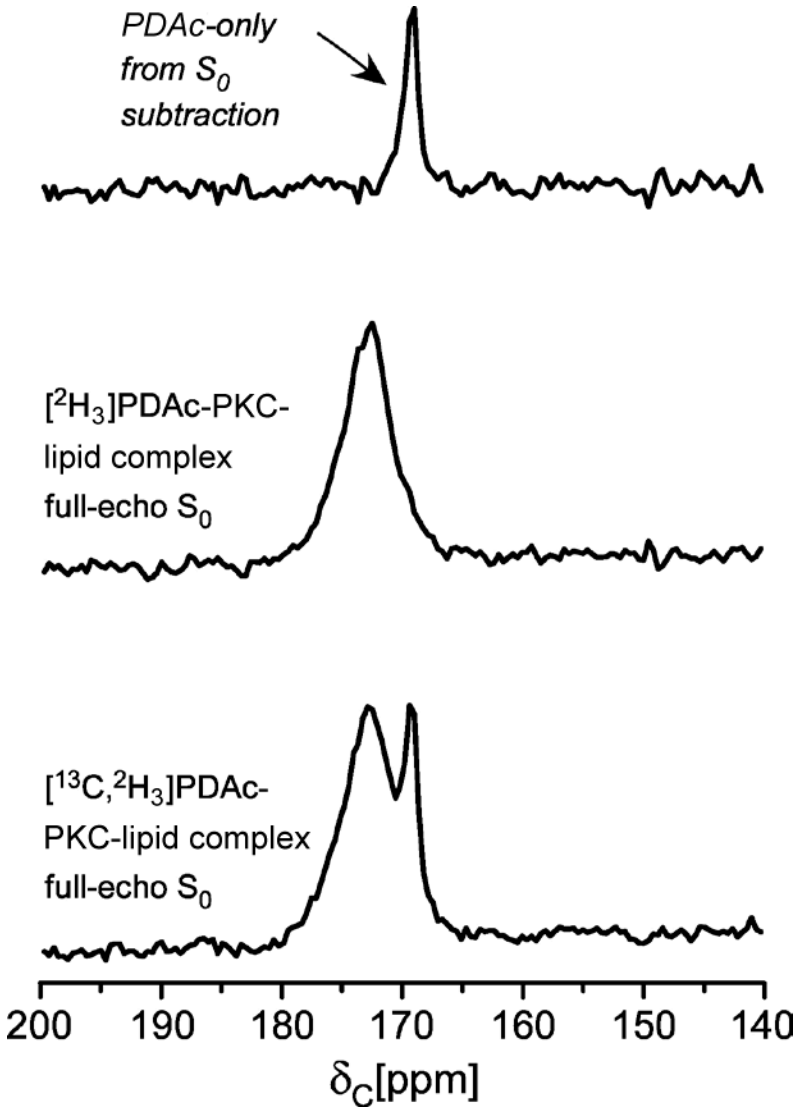

Figure S1. Spectral assignment of the PDAc ^{13}C label among natural-abundance carbonyl contributions from the lipid-protein-PDAc complex. The PDAc-only contribution (top) to the full ^{13}C spectrum of the lipid-peptide-PDAc complex was obtained by subtraction of the CPMAS-echo spectrum of the non-^{13}C labeled PDAc complex, [$^2H_3$]PDAc (middle), from the ^{13}C-labeled PDAc complex (bottom). Each spectrum is an 160-T_r CPMAS-echo spectrum obtained from magic-angle spinning at 7143 Hz. The middle spectrum is the result of accumulation of 36,000 scans, and the bottom spectrum is the result of accumulation of 62,000 scans.

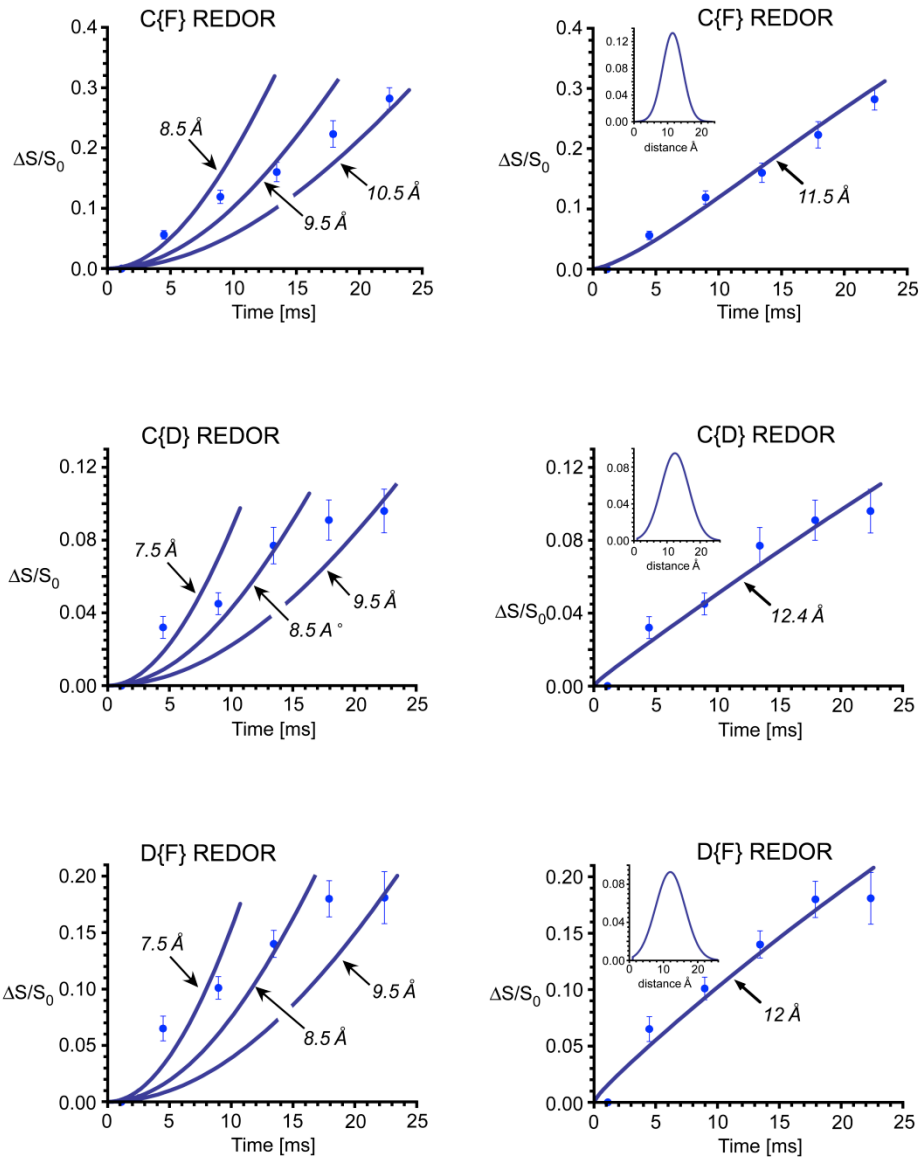

Figure S2. REDOR dephasing data for the [^{19}F,^{13}C,^{2}H$_3$]bryolog-PKCδ-C1b-phospholipid complex compared with REDOR curves of single distances (left) and Gaussian distributions of distances (right) with the corresponding Gaussian functions shown in the insets. Clearly, the REDOR dephasing data do not fit to single-distance REDOR curves (left), but can fit to REDOR curves with a broad Gaussian distribution of distances (right).[33]

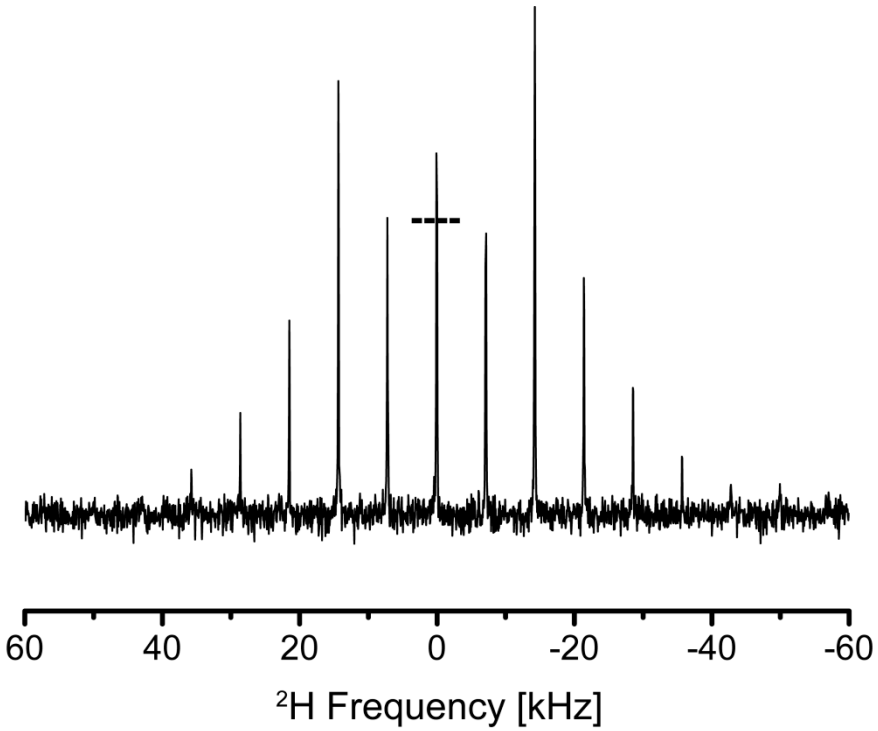

Figure S3. The ^{2}H Hahn echo spectrum of the [^{19}F,^{13}C,$^{2}H_3$]bryolog-PKC-lipid complex with an 8-sec recycle delay. The spectrum predominantly displays a Pake pattern, corresponding to the immobile PKC-bound bryolog. The centerband is slightly higher than that of a Pake pattern (dotted lines), indicating minor mobile bryolog components. The spectrum was the result of accumulation of 13,000 scans with magic-angle spinning at 7143 Hz.

```
STANDARD PROTON PARAMETERS

 Archive directory:
   /export/home/stavenes/vnmrsys/data
 Sample directory:

 File: DSIV.250.hplc.1H

Pulse Sequence: s2pul
Solvent: CDCl3

 Pulse 48.8 degrees
 Acq. time 4.000 sec
 Width 8000.0 Hz
 16 repetitions
OBSERVE    H1, 499.7485737 MHz
DATA PROCESSING
FT size 65536
Total time 8 min
```

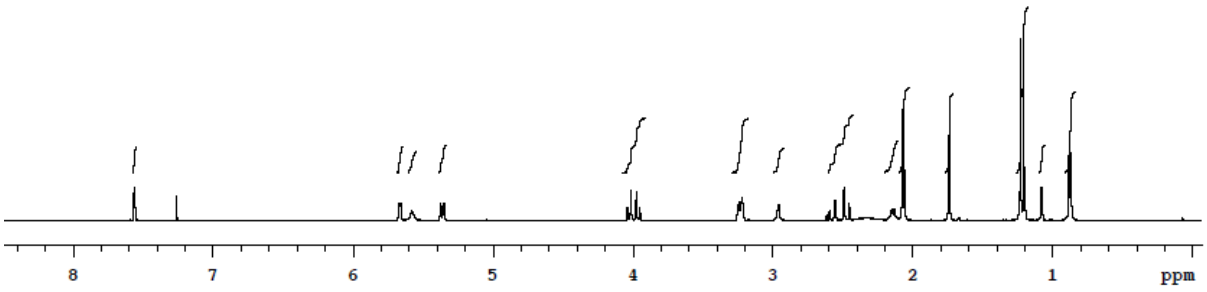

Figure S4. ^{1}H NMR spectrum of [^{13}C,$^{2}H_3$]PDAc **4.**

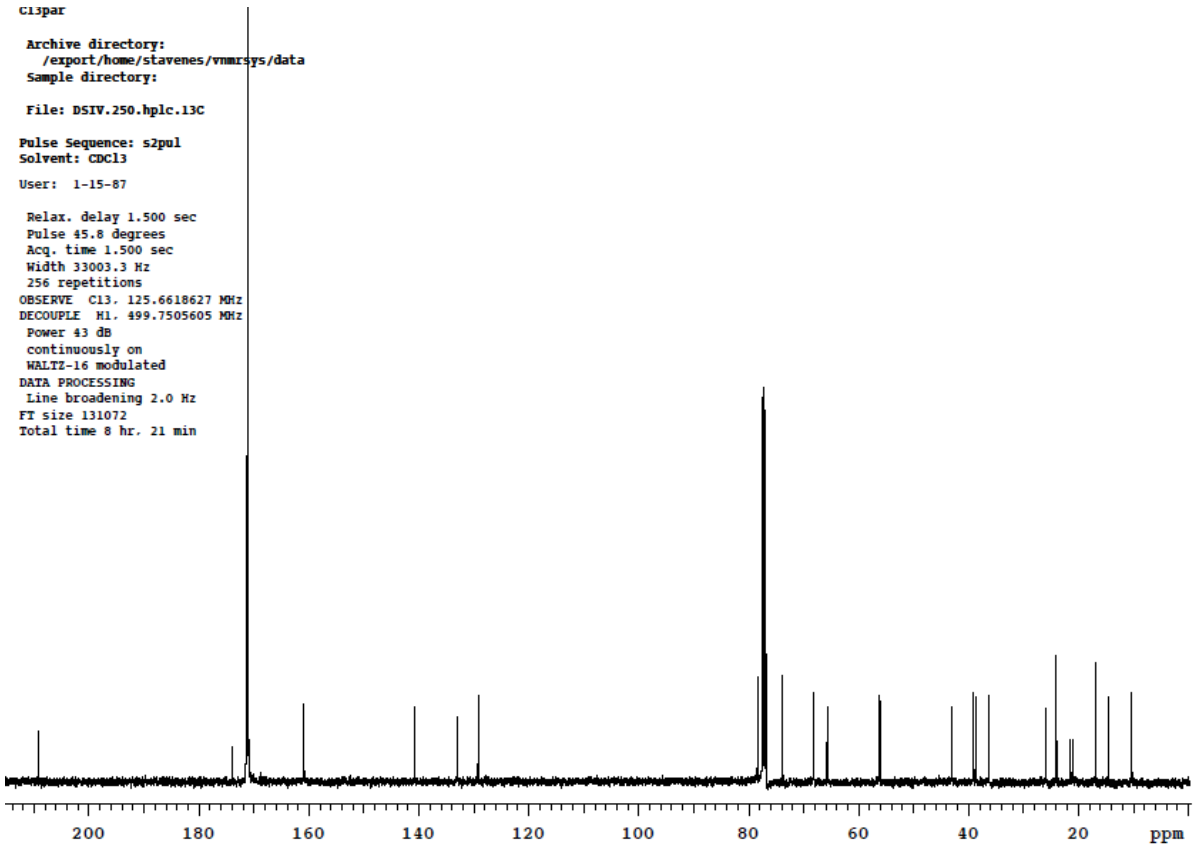

Figure S5. ^{13}C NMR spectrum of [^{13}C,$^{2}H_3$]PDAc **4.**

Supplementary References

(1) Shindo, M.; Irie, K.; Nakahara, A.; Ohigashi, H.; Konishi, H.; Kikkawa, U.; Fukuda, H.; Wender, P. A. Toward the identification of selective modulators of protein kinase C (PKC) isozymes: establishment of a binding assay for PKC isozymes using synthetic C1 peptide receptors and identification of the critical residues involved in the phorbol ester binding. *Bioorg. Med. Chem.* **2001,** *9*, 2073-2081.

(2) Irie, K.; Nakahara, A.; Nakagawa, Y.; Ohigashi, H.; Shindo, M.; Fukuda, H.; Konishi, H.; Kikkawa, U.; Kashiwagi, K.; Saito, N. Establishment of a binding assay for protein kinase C isozymes using synthetic C1 peptides and development of new medicinal leads with protein kinase C isozyme and C1 domain selectivity. *Pharmacol. Ther.* **2002,** *93*, 271-281.

(3) Gullion, T.; Schaefer, J. Rotational-echo double-resonance NMR. *J. Magn. Reson.* **1989,** *81*, 196-200.

(4) Gullion, T.; Schaefer, J. Detection of weak heteronuclear dipolar coupling by rotational-echo double-resonance nuclear magnetic resonance. *Adv. Magn. Reson.* **1989,** *13*, 57-83.

(5) Morcombe, C. R.; Zilm, K. W. Chemical shift referencing in MAS solid state NMR. *J. Magn. Reson.* **2003,** *162*, 479-486.

(6) Stueber, D.; Mehta, A. K.; Chen, Z. Y.; Wooley, K. L.; Schaefer, J. Local order in polycarbonate glasses by $^{13}C\{^{19}F\}$ rotational-echo double-resonance NMR. *J. Polym. Sci., Part B: Polym. Phys.* **2006,** *44*, 2760-2775.

(7) Gullion, T.; Baker, D. B.; Conradi, M. S. New, compensated Carr-Purcell sequences. *J. Magn. Reson.* **1990,** *89*, 479-484.

(8) Gullion, T.; Schaefer, J. Elimination of resonance offset effects in rotational-echo, double-resonance NMR. *J. Magn. Reson.* **1991,** *92*, 439-442.

(9) Mueller, K. T.; Jarvie, T. P.; Aurentz, D. J.; Roberts, B. W. The REDOR transform: direct calculation of internuclear couplings from dipolar-dephasing NMR data. *Chem. Phys. Lett.* **1995,** *242*, 535-542.

(10) Schmidt, A.; McKay, R. A.; Schaefer, J. Internuclear distance measurement between deuterium (I=1) and a spin-1/2 nucleus in rotating solids. *J. Magn. Reson.* **1992,** *96*, 644-650.

(11) Schmidt, A.; Kowalewski, T.; Schaefer, J. Local packing in glassy polycarbonate by carbon-deuterium REDOR NMR. *Macromolecules* **1993,** *26*, 1729-1733.

(12) Ryckbosch, S. M.; Wender, P. A.; Pande, V. S. Molecular dynamics simulations reveal ligand-controlled positioning of a peripheral protein complex in membranes. *Nat. Commun.* **2017,** *8*, 6.

(13) Wang, J. M.; Wolf, R. M.; Caldwell, J. W.; Kollman, P. A.; Case, D. A. Development and testing of a general AMBER force field. *J. Comput. Chem.* **2004,** *25*, 1157-1174.

(14) Wang, J. M.; Wang, W.; Kollman, P. A.; Case, D. A. Automatic atom type and bond type perception in molecular mechanical calculations. *J. Mol. Graph. Model.* **2006,** *25*, 247-260.

(15) da Silva, A. W. S.; Vranken, W. F. ACPYPE-AnteChamber PYthon Parser interfacE. *BMC Res. Notes* **2012,** *5*, 367.

(16) Jambeck, J. P. M.; Lyubartsev, A. P. Another piece of the membrane puzzle: extending Slipids further. *J. Chem. Theory Comput.* **2013,** *9*, 774-784.

(17) Martinez, L.; Andrade, R.; Birgin, E. G.; Martinez, J. M. PACKMOL: a package for building initial configurations for molecular dynamics simulations. *J. Comput. Chem.* **2009,** *30*, 2157-2164.

(18) Hess, B.; Kutzner, C.; van der Spoel, D.; Lindahl, E. GROMACS 4: algorithms for highly efficient, load-balanced, and scalable molecular simulation. *J. Chem. Theory Comput.* **2008,** *4*, 435-447.

(19) Shirts, M.; Pande, V. S. Screen savers of the world unite! *Science* **2000,** *290*, 1903-1904.

(20) Lindorff-Larsen, K.; Piana, S.; Palmo, K.; Maragakis, P.; Klepeis, J. L.; Dror, R. O.; Shaw, D. E. Improved side-chain torsion potentials for the Amber ff99SB protein force field. *Proteins: Struct. Funct. Bioinform.* **2010,** *78*, 1950-1958.

(21) Jorgensen, W. L.; Chandrasekhar, J.; Madura, J. D.; Impey, R. W.; Klein, M. L. Comparison of simple potential functions for simulating liquid water. *J. Chem. Phys.* **1983,** *79*, 926-935.

(22) Parrinello, M.; Rahman, A. Polymorphic transitions in single crystals: a new molecular dynamics method. *J. Appl. Phys.* **1981,** *52*, 7182-7190.

(23) Hess, B.; Bekker, H.; Berendsen, H. J. C.; Fraaije, J. LINCS: a linear constraint solver for molecular simulations. *J. Comput. Chem.* **1997,** *18*, 1463-1472.

(24) Darden, T.; York, D.; Pedersen, L. Particle mesh Ewald: an *N*•Log(*N*) method for Ewald sums in large systems. *J. Chem. Phys.* **1993,** *98*, 10089-10092.

(25) Beauchamp, K. A.; Bowman, G. R.; Lane, T. J.; Maibaum, L.; Haque, I. S.; Pande, V. S. MSMBuilder2: modeling conformational dynamics on the picosecond to millisecond scale. *J. Chem. Theory Comput.* **2011,** *7*, 3412-3419.

(26) Zhou, T.; Caflisch, A. Distribution of reciprocal of interatomic distances: a fast structural metric. *J. Chem. Theory Comput.* **2012,** *8*, 2930-2937.

(27) Harrigan, M. P.; Shukla, D.; Pande, V. S. Conserve water: a method for the analysis of solvent in molecular dynamics. *J. Chem. Theory Comput.* **2015,** *11*, 1094-1101.

(28) Gu, C.; Chang, H. W.; Maibaum, L.; Pande, V. S.; Carlsson, G. E.; Guibas, L. J. Building Markov state models with solvent dynamics. *BMC Bioinformatics* **2013,** *14(Suppl 2)*, S8.

(29) Schwantes, C. R.; Pande, V. S. Improvements in Markov state model construction reveal many non-native interactions in the folding of NTL9. *J. Chem. Theory Comput.* **2013,** *9*, 2000-2009.

(30) Sculley, D. Web-scale k-means clustering. In *Proceedings of the 19th International Conference on World Wide Web*; ACM: New York, 2010; pp 1177-1178.

(31) Nuske, F.; Keller, B. G.; Perez-Hernandez, G.; Mey, A.; Noe, F. Variational approach to molecular kinetics. *J. Chem. Theory Comput.* **2014,** *10*, 1739-1752.

(32) McGibbon, R. T.; Pande, V. S. Variational cross-validation of slow dynamical modes in molecular kinetics. *J. Chem. Phys.* **2015,** *142*, 124105.

(33) Yang, H. Solid-state NMR study of the tertiary structure of the peptidoglycan of *Enterococcus faecalis* and the structures of phorbol diacetate and bryostatin bound to protein kinase Cδ C1b domain. Ph.D. Dissertation, Department of Chemistry, Washington University, St. Louis, MO, 2015.